Autocatalysis

DOI: 10.1002/ange.201005246

Amplified Detection of DNA through an Autocatalytic and Catabolic DNAzyme-Mediated Process**

*Fuan Wang, Johann Elbaz, Carsten Teller, and Itamar Willner**

The amplified detection of DNA has spurred substantial research efforts, and numerous electrical,[1] optical,[2] or microgravimetric[3] amplified DNA sensors have been reported. The amplification approaches included the conjugation of enzymes,[4] catalytic nanoparticles,[5] or molecular catalysts[6] to the DNA recognition complex or the tethering of the recognizing reporter nucleic acid to a label that, upon dissolution, leads to numerous redox-active reporter units as a result of a single sensing event.[7] Catalytic nucleic acids (DNAzymes or ribozymes) have found growing interest as amplifying labels for biosensing events.[8] The easy synthetic preparation of DNAzymes and the reduced nonspecific adsorption of DNAzymes make catalytic nucleic acids attractive reporter units. For example, the horseradish peroxidase mimicking DNAzyme[9] was used extensively to amplify DNA detection,[10] to follow enzymatic reactions,[11] and to follow the formation of aptamer–substrate complexes.[12] Similarly, ion-dependent DNAzymes were used for the specific amplified sensing of ions.[13] However, the real challenge in DNA detection lies in the development of methods that can substitute the polymerase chain reaction (PCR). In particular, the development of isothermal amplification systems that are activated upon sensing of the analyte nucleic acid is a challenging goal. DNA sensor systems that implement DNAzymes as amplifying labels have been designed.[14] The use of DNA-based machines has recently been suggested as a means to stimulate the autonomous replication of a catalytic reporter as the result of DNA sensing.[15] For example, the autonomous replication–scission–displacement process of the horseradish peroxidase mimicking DNAzyme generated by polymerase, dNTPs, and a nicking enzyme was reported as an effective amplified replication system as a result of the recognition of the DNA analyte on a predesigned nucleic acid track.[16] Also, the rolling circle amplification process was applied to detect DNA analytes through the autonomous synthesis of a horseradish peroxidase mimicking DNAzyme repeat unit that acted as the biocatalytic amplifier.[14c] Such systems require, however, protein-based enzymes (polymerases or nicking enzymes) as biocatalytic amplifiers.

Herein we report on the protein-free, isothermal, and autocatalytic detection of DNA by using the E6 Mg^{2+}-dependent DNAzyme[17] as a biocatalyst. The cleavage of a fluorophore-quencher-functionalized ribonucleotide-containing substrate by the DNAzyme leads to the generation of higher fluorescence, which provides the readout signal for the analytical platform.

Figure 1 A depicts the DNAzyme-catalyzed, non-autocatalytic analysis of target DNA **1** by the Mg^{2+}-dependent DNAzyme. The system includes two subunits, **2** and **3**; subunit **3** forms a hairpin structure that includes only the base sequence complementary to the analyte in the loop region I and the stem domain V. The subunits **2** and **3** contain the base sequence that corresponds to the Mg^{2+}-dependent DNAzyme in the domains II and III, as well as nucleic acid tethers IV and V that exhibit mutual base complementarities. Additionally, the ribonucleotide-containing substrate **4**, which is modified

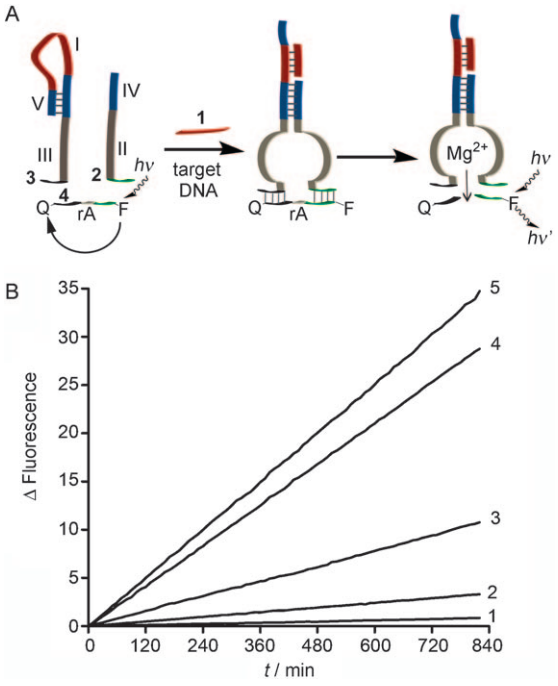

Figure 1. A) Schematic representation of the analyte-induced DNAzyme assembly and the subsequent hydrolysis of the fluorophore and quencher-labeled adenosine ribonucleotide (rA) containing substrate. B) Time-dependent changes in the fluorescence of the non-autocatalytic nucleic acid sensing with target concentrations of: 1) 0 M, 2) 1×10^{-9} M, 3) 1×10^{-8} M, 4) 1×10^{-7} M, and 5) 1×10^{-6} M. The initial fluorescence value at $t=0$ min was subtracted from the curves.

[*] Dr. F. Wang, J. Elbaz, Dr. C. Teller, Prof. I. Willner
Institute of Chemistry, The Hebrew University of Jerusalem
Jerusalem 91904 (Israel)
Fax: (+972) 2652-7715
E-mail: willnea@vms.huji.ac.il

[**] Financial support by the EU ECCell project, the Israel Science Foundation (Converging Technologies fellowship to J.E.), and the Minerva foundation (postdoctoral fellowship to C.T.) is gratefully acknowledged. We thank Prof. G. von Kiedrowski for helpful comments.

Supporting information for this article is available on the WWW under http://dx.doi.org/10.1002/anie.201005246.

at its 3′ and 5′ ends with a fluorophore and a quencher, respectively, is included in the system. As the domain V of subunit **3** is blocked by the hairpin stem region, the supramolecular structure of the DNAzyme (subunits **2** and **3**) cannot be formed, and thus the substrate **4** is not cleaved. Upon interaction of the components with the analyte **1**, the hairpin structure is opened, thereby giving rise to the assembly of the units **2** and **3** into the active E6-derived DNAzyme structure. The synergistic binding of the substrate **4** to the DNAzyme structure results in the hydrolytic cleavage of **4** in the presence of Mg^{2+} ions. The limited duplex stability of the cleaved substrate leads to the release of the product units from the DNAzyme structure and allows the continuous scission of the substrate. The scission of **4** results in the generation of a higher fluorescence intensity that provides the optical readout signal for the sensing of the analyte.

Figure 1 B shows the time-dependent fluorescence changes that allow for the non-autocatalytic sensing of different concentrations of the analyte **1**. Control experiments show that there is little to no background reaction of the DNAzyme in the absence of the nucleic acid target, thus indicating that no active DNAzyme was formed. In Figure 1 B, curves 1 to 5 show that the DNAzyme is activated in the presence of the analyte **1**, and as the concentration of **1** increases, the fluorescence intensifies. The system enabled the detection of **1** with a sensitivity that corresponded to 1×10^{-9} M. The sensitivity values reported herein correspond to fluorescence intensities that are $\geq 10\,\%$ higher than the intensity of the corresponding fluorescence background value.

The autocatalytic system for the amplified detection of the analyte **1** by the Mg^{2+}-dependent DNAzyme is depicted in Figure 2 A. The subunits **2** and **3** are preserved in similar structures as in the non-autocatalytic sensing platform. The only difference that is introduced is the use of the nucleic acid hairpin **5** as the substrate for the DNAzyme. The sequence of **5** contains two domains, VI and VII, where domain VI represents the hairpin loop that includes an adenine ribonucleotide in the single-stranded loop that acts as the substrate for the Mg^{2+}-dependent DNAzyme. The stem region, domain VII, contains the sequence of the target analyte DNA **1**, but the stable hairpin structure of **5** preserves this sequence in a sequestered structure, thus prohibiting the activation of the DNAzyme. Additionally, a fluorophore and a quencher are tethered to the 3′ and 5′ ends of the stem region, respectively, which leads to quenching of the fluorescence of the fluorophore in the hairpin. In the presence of analyte **1**, the hairpin structure of subunit **3** is opened, thus generating the active DNAzyme structure that synergistically binds the hairpin substrate **5**. The catalyzed cleavage of the substrate **5** leads to two fragments **6** and **7** that lack sufficient base-pairing stability and dissociate in solution. The fluorophore-labeled nucleic acid fragment **7** provides the read-out signal of the detection system. The released activator unit **6**, however, includes the base sequence of the analyte, and thus opens subunit **3**. This process leads to the enhanced formation of the DNAzyme structure and the increased cleavage of **5**, with the concomitant generation of a fluorescent signal of higher intensity. Thus, in the presence of the analyte **1**, the autonomous, autocatalytic accumulation of the analyte sequence is activated, which leads to the effective generation of the Mg^{2+}-dependent DNAzyme units, and the resulting fluorescence increases. Control experiments showed that small to no fluorescence changes were observed in the absence of the analyte. This behavior is maintained for time intervals up to 14 h, thus implying that the coincidental

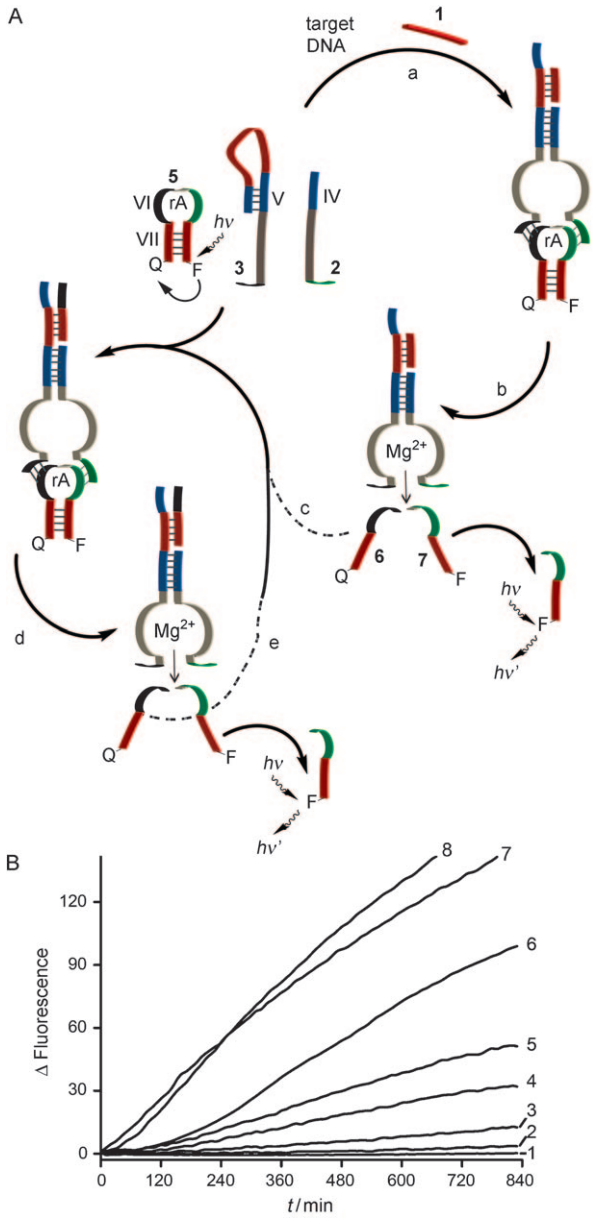

Figure 2. A) Schematic representation of the analyte-induced DNAzyme assembly and the sensing process: a) target recognition and assembly of the DNAzyme, b) cleavage of the substrate **5** and release of the activator unit **6**, c)–e) autocatalytic catabolic generation cycle triggered by the activator-unit-induced assembly of the DNAzyme. B) Time-dependent fluorescence changes of the autocatalytic nucleic acid sensing in the presence of different target concentrations: 1) 0 M, 2) 1×10^{-12} M, 3) 1×10^{-11} M, 4) 1×10^{-10} M, 5) 1×10^{-9} M, 6) 1×10^{-8} M, 7) 1×10^{-7} M, and 8) 1×10^{-6} M. The initial fluorescence value at $t=0$ min was subtracted from the curves.

activation of the autocatalytic process by any trace amount of open **5** (in the absence of the target analyte) does not occur.

Figure 2B shows the time-dependent fluorescence changes upon analyzing different concentrations of **1** by the amplifying, autocatalytic generation of the analyte sequence. As the concentration of the analyte increases, the fluorescence intensity generated by the system also increases. The system enables the detection of the target **1** with a detection limit that corresponds to 1×10^{-12} M, a value that indicates a sensitivity that is 1000 times higher than that of the non-autocatalytic DNAzyme-amplified system. Furthermore, the time-dependent background fluorescence intensities of the systems were practically unchanged (±2.0% in the absence of target **1**; see Figures S1 and S2 in the Supporting Information). It should be noted that the autocatalytic sensing system shown in Figure 2A contains substantial structural and functional information. For the appropriate operation of the system, the following requirements need to be met: 1) The hybridization of the stem region of hairpin **3** should be sufficiently strong to eliminate the formation of the DNAzyme structure in the absence of analyte **1**, that is, any activation of the autocatalytic process in the absence of the analyte would generate an undesired background signal. 2) Hybridization of the analyte **1** with the recognition sequence in the loop of hairpin **3** should generate a sufficiently stable duplex that opens the stem region of **3**, thus activating the autocatalytic process. 3) The hairpin **5** that provides the readout signal requires specific design: as it includes the analyte sequence as a built-in component, this sequence must be fully hybridized and sequestred in the stem region of hairpin **5** to eliminate the opening of hairpin **3**. 4) The activation of the entire autocatalytic amplification process is based on the delicate stabilities of the duplexes in the different components; therefore, the temperature at which the process is activated plays a major role in the optimization of the system. To meet these requirements, the structures of the different nucleic acids contained in the system and the temperature at which autocatalytic amplification was activated, had to be optimized. The optimized system should give zero (or close to zero) background signal (small to no fluorescence changes), while a large intensity change of the fluorescence signal in the presence of the analyte should be generated. Table 1 shows four different hairpin sequences for hairpin **3** (**3a–d**) that include 4, 5, 6, and 8 base pairs in the stem region, with **5** used as the readout substrate. Based on the changes in the fluorescence intensity of the systems in the absence or presence of the analyte, we found that **3c** gives the best analytical results (for detailed experimental results, see Figure S1 in the Supporting Information). Similarly, the structure of hairpin **5**, which generates the readout signal, was optimized by using three different fluorophore–quencher hairpin substrates (**5a–5c**, see Table 1). By using the optimized subunit **3c** we found that hairpin **5b** gave the best analytical performance for zero background signal in the absence of the analyte and larger fluorescence changes in the presence of the analyte (for detailed experimental results, see Figure S2 in the Supporting Information). Finally, the temperature at which the autocatalytic process is activated was optimized and the performance of the system was examined at 20°C, 25°C, and 32°C. We found that the activation of the system at 25°C gives the best results (for experimental details, see Figure S3 in the Supporting Information).

Table 1: Optimization of the nucleic acid sequences **3** and **5**.

Sequences		ΔF_0[a]	ΔF_1[a]
3a	5′ AC TCT GTC CGA GTC TTC CAC CCA TGT TAC TCT 3′	53	289
3b	5′ GAC TCT GTC CGA GTC TTC CAC CCA TGT TAC TCT 3′	26	197
3c	5′ A GAC TCT GTC CGA GTC TTC CAC CCA TGT TAC TCT 3′	0	127
3d	5′ GAA GAC TCT GTC CGA GTC TTC CAC CCA TGT TAC TCT 3′	0	42
5a	5′ Q-GT GGA CAG AGT ATrA GGA TAT CAA TTT TTT TTT TTT AGT CCA C-F 3′	31	262
5b	5′ Q-GCT GGA CAG AGT ATrA GGA TAT CAA TTT TTT TTT TTT AGT CCA GC-F 3′	0	131
5c	5′ Q-G GCT GGA CAG AGT ATrA GGA TAT CAA TTT TTT TTT TTT AGT CCA GCC-F 3′	0	94

[a] ΔF_1 and ΔF_0 represent the change in the fluorescence after 12 h in the presence or absence, respectively, of the DNA target **1** in the autocatalytic system.

It should be noted that the autocatalytic system for the detection of the analyte represents an optimized sensing platform, which can analyze any target DNA without much further optimization of the established system. Figure 3A outlines the general method for the analysis of a different target DNA (e.g. **9**) by the autocatalytic amplification system. The only added component is the DNAzyme subunit **8**, which contains the appropriate loop domain for the respective target analyte in the hairpin that blocks the assembly of the DNAzyme. Hence, the stem hairpin **8** is identical to the optimized stem in **3**. The analytical process includes a sensing module (non-autocatalytic process) that initiates the autocatalytic module. The assembly of the DNAzyme upon sensing of **9** results in the cleavage of **5**. The quencher-labeled fragment **6** allows the opening of the hairpin-blocking subunit **3**, thus activating the autocatalytic cycle as described above. Figure 3B illustrates the analysis of a new target (**9**) by the general platform described in Figure 3A upon the addition of only one extra component (**8**). Again, a very low background signal (±3.5%) is observed in the absence of the target nucleic acid **9**.

In conclusion, we have developed a protein-free nucleic acid sensing system based on the Mg^{2+}-dependent DNAzyme E6. The DNAzyme was divided into two subunits, one of which was sequestered by a hairpin structure that prevented the assembly of the catalytically active DNAzyme. The addition of the nucleic acid analyte allowed the opening of this hairpin and facilitated the assembly of the DNAzyme. The first stage of development of the sensing platform employed a linear nucleic acid substrate that was labeled at each end with a fluorophore and a quencher, respectively. This design allowed for the non-autocatalytic sensing of the nucleic acid target with a sensitivity of 1 nM. Further development of the system led to a detection platform that used an autocatalytic process to amplify the sensing event.

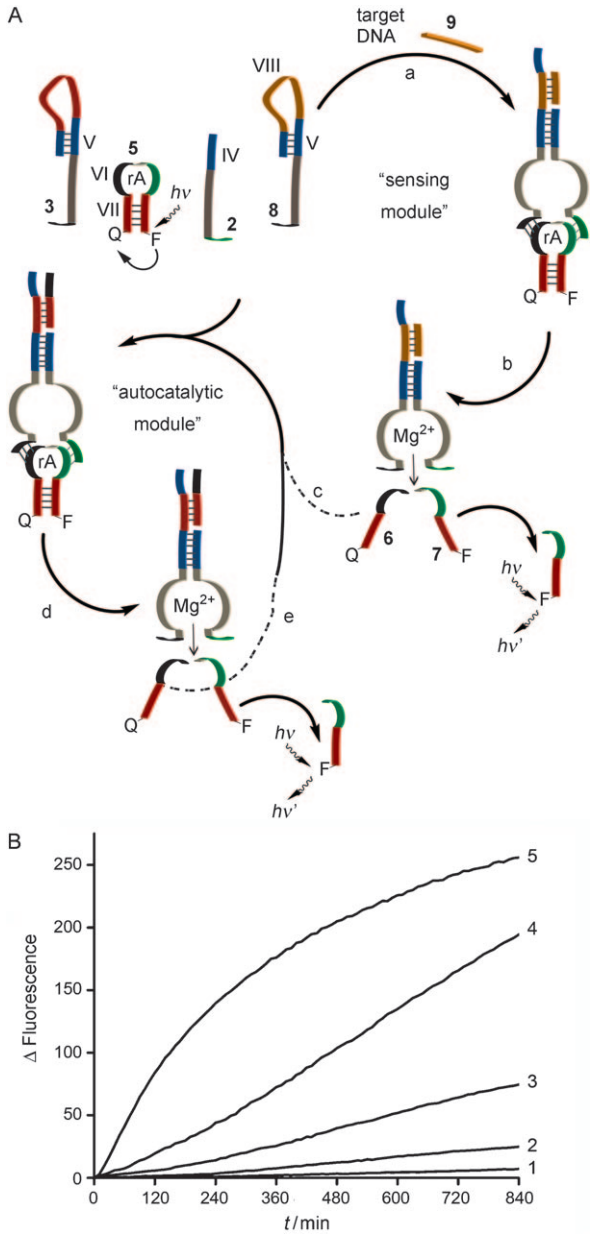

Figure 3. A) Schematic representation of the general analyte-sensing platform: the sensing module process (a–b) initiates the autocatalytic module process (c–e). B) Time-dependent fluorescence changes upon the activation of the general sensing platform. The curves show the change in fluorescence in the presence of different concentrations of the DNA target **9**: 1) 0 M, 2) 1×10^{-12} M, 3) 1×10^{-10} M, 4) 1×10^{-8} M, 5) 1×10^{-7} M. The initial fluorescence value at $t=0$ min was subtracted from the curves.

This was achieved by using a hairpin substrate that included a sequestered structure with the analyte sequence. The DNAzyme-catalyzed scission of the hairpin rendered this stem structure unstable, and released another copy of the nucleic acid target sequence. Thus, very low concentrations of the analyte were sufficient to initiate an autocatalytic cascade. We achieved a significant improvement of the detection limit down to 1 pM—a 1000-fold improvement compared to the non-autocatalytic system depicted in Figure 1. Although the sensitivity of this system exceeds DNA-templated detection platforms that rely on purely chemical, non-enzymatic reactions,[18] it is still approximately 100-fold less efficient than other isothermal DNA-based machines.[14c,16] However, the advantages of the current sensing platform include the fact that it is free from added protein enzymes. The DNAzyme used in the present study exhibits a relatively low turnover rate, thus suggesting that the application of DNAzymes with enhanced activities could improve the performance of this sensing platform.[14a]

Experimental Section

Nucleic acid sequences used herein (5′ to 3′, F = FAM fluorophore, Q = black hole quencher 1, rA = adenine ribonucleotide):

1	GGA CAG AGT
2	GAT ATC AGC GAT GAA GAC TC
3	AGA CTC TGT CCG AGT CTT CCA CCC ATG TTA CTC T
4	Q-AGA GTA TrAG GAT ATC-F
5	Q-GCT GGA CAG AGT ATrA GGA TAT CAA TTT TTT TTT TTT AGT CCA GC-F
8	AGA CTC TCA TCA CAC AAT GAG TCT TCC ACC CAT GTT ACT CT
9	ATT GTG TGA TGA

All assays were performed in 10 mM 2-[4-(2-hydroxyethyl)-1-piperazinyl]ethanesulfonic acid (HEPES) buffer at pH 7.4 containing 1 M NaCl, 20 mM $MgCl_2$, 0.3 μM of the respective DNAzyme subunits, and 0.2 μM of the respective substrate as described in the figure captions. The mixture was heated to 90 °C for 5 min and instantly cooled down to 25 °C for 1 hour. Then, different concentrations of the target DNA **1** were added to the solutions at 25 °C.

Received: August 22, 2010
Published online: November 16, 2010

Keywords: autocatalysis · DNA · DNAzymes · fluorescence · sensors

[1] a) W. Tan, K. Wang, T. J. Drake, *Curr. Opin. Chem. Biol.* **2004**, *8*, 547–553; b) C. Fan, K. W. Plaxco, A. J. Heeger, *Proc. Natl. Acad. Sci. USA* **2003**, *100*, 9134–9137.
[2] a) Y. Lu, J. Liu, *Curr. Opin. Biotechnol.* **2006**, *17*, 580–588; b) N. K. Navani, Y. Li, *Curr. Opin. Chem. Biol.* **2006**, *10*, 272–281.
[3] a) F. Lucarelli, S. Tombelli, M. Minunni, G. Marrazza, M. Mascini, *Anal. Chim. Acta* **2008**, *609*, 139–159; b) Y. Weizmann, F. Patolsky, I. Willner, *Analyst* **2001**, *126*, 1502–1504.
[4] F. Patolsky, A. Lichtenstein, I. Willner, *Nat. Biotechnol.* **2001**, *19*, 253–257.
[5] R. Polsky, R. Gill, L. Kaganovsky, I. Willner, *Anal. Chem.* **2006**, *78*, 2268–2271.
[6] a) J. Li, H. T. Ng, A. Cassell, W. Fan, H. Chen, Q. Ye, J. Koehne, J. Han, M. Meyyappan, *Nano Lett.* **2003**, *3*, 597–602; b) L. Zhou, J. Yang, C. Estavillo, J. D. Stuart, J. B. Schenkman, J. F. Rusling, *J. Am. Chem. Soc.* **2003**, *125*, 1431–1436.
[7] N. Zhu, A. Zhang, P. He, Y. Fang, *Analyst* **2003**, *128*, 260–264.
[8] a) M. Famulok, G. Mayer, M. Blind, *Acc. Chem. Res.* **2000**, *33*, 591–599; b) D. M. Kolpashchikov, *ChemBioChem* **2007**, *8*, 2039–2042; c) S. K. Silverman, *Chem. Commun.* **2008**, 3467;

d) S. Sando, T. Sasaki, K. Kanatani, Y. Aoyama, *J. Am. Chem. Soc.* **2003**, *125*, 15720 – 15721.
[9] P. Travascio, Y. F. Li, D. Sen, *Chem. Biol.* **1998**, *5*, 505.
[10] a) D. M. Kolpashchikov, *J. Am. Chem. Soc.* **2008**, *130*, 2934 – 2935; b) J. Elbaz, M. Moshe, B. Shlyahovsky, I. Willner, *Chem. Eur. J.* **2009**, *15*, 3411.
[11] a) Y. Xiao, V. Pavlov, T. Niazov, A. Dishon, M. Kotler, I. Willner, *J. Am. Chem. Soc.* **2004**, *126*, 7430 – 7431; b) W. Li, Z. Liu, H. Lin, Z. Nie, J. Chen, X. Xu, S. Yao, *Anal. Chem.* **2010**, *82*, 1935 – 1941.
[12] a) C. Teller, S. Shimron, I. Willner, *Anal. Chem.* **2009**, *81*, 9114 – 9119; b) J. Elbaz, B. Shlyahovsky, D. Li, I. Willner, *ChemBioChem* **2008**, *9*, 232 – 239.
[13] a) J. Liu, Z. Cao, Y. Lu, *Chem. Rev.* **2009**, *109*, 1948 – 1998; b) J. Elbaz, B. Shlyahovsky, I. Willner, *Chem. Commun.* **2008**, 1569 – 1571.
[14] a) Y. V. Gerasimova, D. M. Kolpashchikov, *Chem. Biol.* **2010**, *17*, 104 – 106; b) E. Mokany, S. M. Bone, P. E. Young, T. B. Doan, A. V. Todd, *J. Am. Chem. Soc.* **2010**, *132*, 1051 – 1059; c) Z. Cheglakov, Y. Weizmann, B. Basnar, I. Willner, *Org. Biomol. Chem.* **2007**, *5*, 223 – 225.
[15] W. Xu, X. Xue, T. Li, H. Zeng, X. Liu, *Angew. Chem.* **2009**, *121*, 6981 – 6984; *Angew. Chem. Int. Ed.* **2009**, *48*, 6849 – 6852.
[16] Y. Weizmann, M. K. Beissenhirtz, Z. Cheglakov, R. Nowarski, M. Kotler, I. Willner, *Angew. Chem.* **2006**, *118*, 7544 – 7548; *Angew. Chem. Int. Ed.* **2006**, *45*, 7384 – 7388.
[17] R. R. Breaker, G. F. Joyce, *Chem. Biol.* **1995**, *2*, 655 – 660.
[18] a) Y. Xu, N. B. Karalkar, E. T. Kool, *Nat. Biotechnol.* **2001**, *19*, 148 – 152; b) T. N. Grossmann, O. Seitz, *J. Am. Chem. Soc.* **2006**, *128*, 15596 – 15597; c) Z. L. Pianowski, N. Winssinger, *Chem. Commun.* **2007**, 3820 – 3822.

